# Spatial and Temporal Variability of Solar Radiation Arriving at the Top of the Atmosphere

## V. M. Fedorov[a] and D. M. Frolov[a], *

*[a]Moscow State University, Moscow, 119899 Russia*
*\*e-mail: denisfrolov@mail.ru*
Received November 20, 2017; revised August 16, 2018; accepted September 20, 2018

**Abstract**—Based on the previously calculated insolation of the Earth, we determine the variations in solar radiation arriving at the top of the atmosphere, which are mainly connected with changes in the inclination of Earth's rotation axis due to precession and nutation. The amplitudes of semiannual and hemispheric variations in solar radiation arriving at the top of the atmosphere were calculated. The results can be used in precise calculations of the radiative balance of Earth and its surface and atmosphere.

## INTRODUCTION

Solar radiation is the main source of energy that determines the radiative thermal balance of Earth. For the interval between the years 1900 and 2100, the annual insolation at the top of the atmosphere (TOA) of Earth averages $5.49 \cdot 10^{24}$ J [3, 8] or $1.0777 \cdot 10^{10}$ J/m². This insolation is not constant; it changes in both time and space. Variations in the radiative energy coming to Earth are mostly determined by two causes of different physical nature. One of these causes is connected with changes in solar radiation intensity. The other cause, determining the change in energy coming to Earth, is the processes of celestial mechanics; they induce changes in the orbital elements of Earth [4–6] and the inclination of its rotation axis. In this paper, we consider spatial and temporal variations connected with the processes of celestial mechanics. Solar activity variations are ignored.

The TOA is a conventional surface, which is a reference for the energy (radiative and thermal) balance of Earth and its surface and atmosphere [2, 16, 17, 25–27]. When calculating the balance, different (from 340 to 342 W/m²), though stationary, values of the energy characteristic of the TOA are assumed (usually, it is the solar radiation intensity) [23, 24, 27].

Our calculations show that solar radiation, arriving at the TOA, experiences changes in both time and space [7, 9–14]. Both long-term trends and small periodic variations are distinguishable. The purpose of the paper is to estimate changes in the initial conditions for radiative balance calculations in the case, when these changes are connected with variations in solar radiation arriving at the TOA and these variations are induced by perturbations in the orbital motion of Earth and the inclination of its rotation axis. To char-

acterize the initial conditions for energy balance calculations, we used a value of the solar radiation arriving at the TOA for a tropical year (expressed in J/m²) rather than its intensity (expressed in W/m²). Variations in the incoming solar radiation at the TOA are analyzed and estimated for the years from 1900 to 2100.

## CALCULATION PROCEDURE

Incoming solar radiation was calculated according to high-accuracy astronomical ephemerides [15, 18] for the entire surface of Earth (in the absence of the atmosphere) for the period from 3000 B.C. to 2999 A.D. To calculate the insolation, we used the following astronomical data as a source: the declination and ecliptic longitude of the Sun, the Earth–Sun distance, and the rate difference between the uniformly passing (mean solar) time and the corrected universal (true solar) time. Earth's surface was approximated by an ellipsoid (the Geodetic Reference System of 1980 or GRS80) with a semimajor axis of 6378137 m and a semiminor axis of 6356752 m. In general, the calculation algorithm can be presented in the following form

$$I_{nm}(\varphi_1, \varphi_2)$$
$$= \int_{t_1}^{t_2} \left( \int_{\varphi_1}^{\varphi_2} \sigma(H, \varphi) \left( \int_{-\pi}^{\pi} \Lambda(H, t, \varphi, \alpha) d\alpha \right) d\varphi \right) dt, \quad (1)$$

where $I$ is incoming solar radiation (J) for an elementary $n$th fragment of the $m$th tropical year, $\sigma$ is the area factor (m²) used to calculate areolar derivative $\sigma(H, \varphi) d\alpha d\varphi$ (i.e., the area of a trapezium-shaped infinitesimal cell of the ellipsoid), $\alpha$ is the hour angle (rad), $\varphi$ is the geographic latitude (rad), $H$ is the altitude of the surface of the ellipsoid with reference to
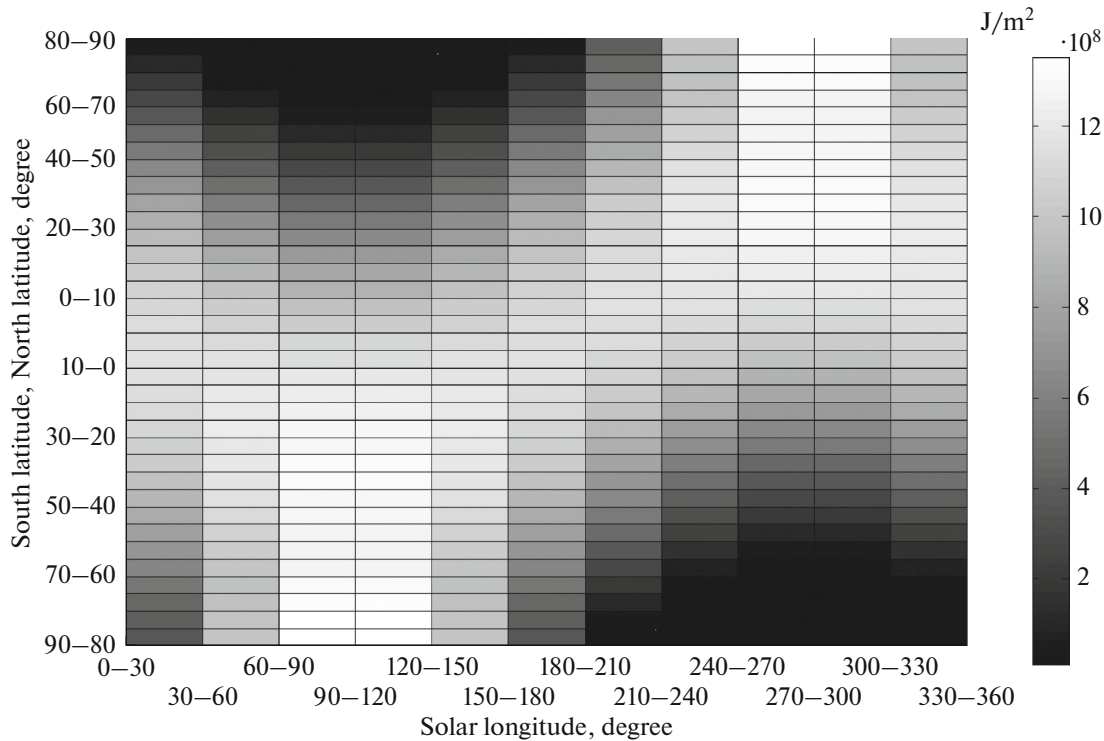
**Fig. 1.** Distribution of the solar radiation arriving at the TOA in the tropical year 2017 (the tropical year 2017 started on March 21 of the calendar year 2017).

Earth's surface (m), $\Lambda(H, \varphi, t, \alpha)$ is the insolation at a specified instant at a given site of the ellipsoid (W/m$^2$), and $t$ is the time (s). The integration steps were 1° in longitude and latitude and 1/360 of the tropical year duration in time [10]. The solar constant (the average perennial value of the total solar irradiance (TSI)) was assumed to be 1361 W/m$^2$ [21]. From the results of calculations for the period from 3000 B.C. to 2999 A.D., the database of solar radiation incoming to the TOA in the latitudinal zones of Earth (5° wide each) was created with a time step of 1/12 of the tropical year duration [19]. The change in solar activity was not included in calculations.

## RESULTS AND DISCUSSION

We calculated the annual values while considering the changes in the parameters of Earth's orbital motion (the Earth–Sun distance, tropical year duration, and rotation axis inclination). The distribution of total solar radiation arriving at the TOA in tropical year 2017 is presented in Fig. 1.

In fact, this surface is permanently changing, which reflects the variations in solar radiation arriving at the TOA determined by perturbations in Earth's orbital motion and the insolation conditions connected with these perturbations. It is these variations that are analyzed in this paper.

The spatial and temporal changes in solar radiation arriving at the TOA for a period of 1900–2100 were analyzed in depth. The performed calculations show that solar radiation arriving at the TOA of Earth for a tropical year is characterized by a rather weak downward trend (Fig. 2).

In the long-term variability of solar radiation arriving at the TOA, considerable year-to-year variations with a period of 2, 3, 8, 11, and 19 years are observed [7, 9–11].

To analyze thoroughly the changes in solar radiation arriving at the TOA, we generated matrices of values of the solar radiation coming to different latitudinal zones (5° wide each) for astronomical months (1/12 of a tropical year duration) for years 1900 and 2100. As a reminder, a tropical year is a time interval between two successive passages of the center of the apparent Sun through the vernal equinox [1]. Then, by subtracting the calculated values of the solar radiation coming to the TOA in 1900 from the corresponding values for 2100, we obtained the matrix of the change in solar radiation arriving at the TOA occurring from 1900 to 2100 (Fig. 3).

In the behavior of the changes revealed for this period, the following features can be distinguished.

(1) No solar radiation comes to latitudinal zones of 80°–90° S for a period of the second to fifth astronomical months of a tropical year. In a latitudinal zone
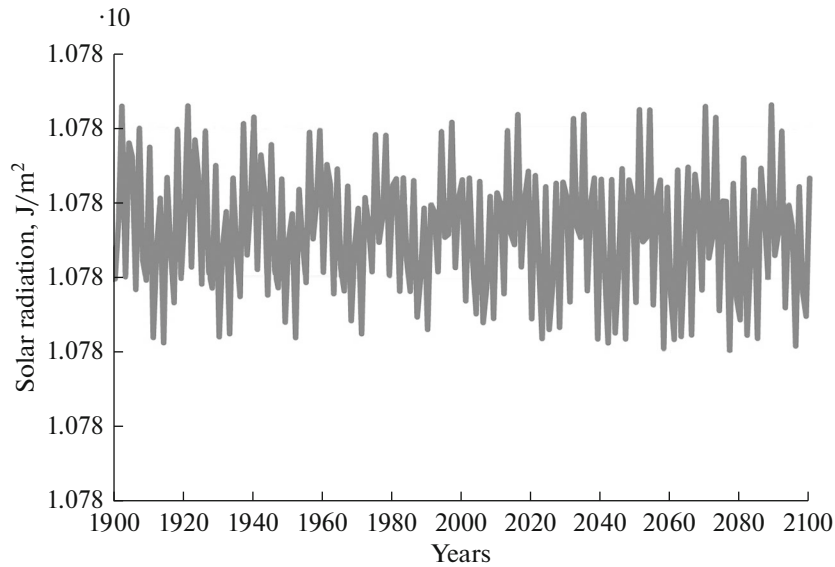
**Fig. 2.** Variations in solar radiation arriving at the TOA for a tropical year in the period from 1900 to 2100 (expressed in $J/m^2$).
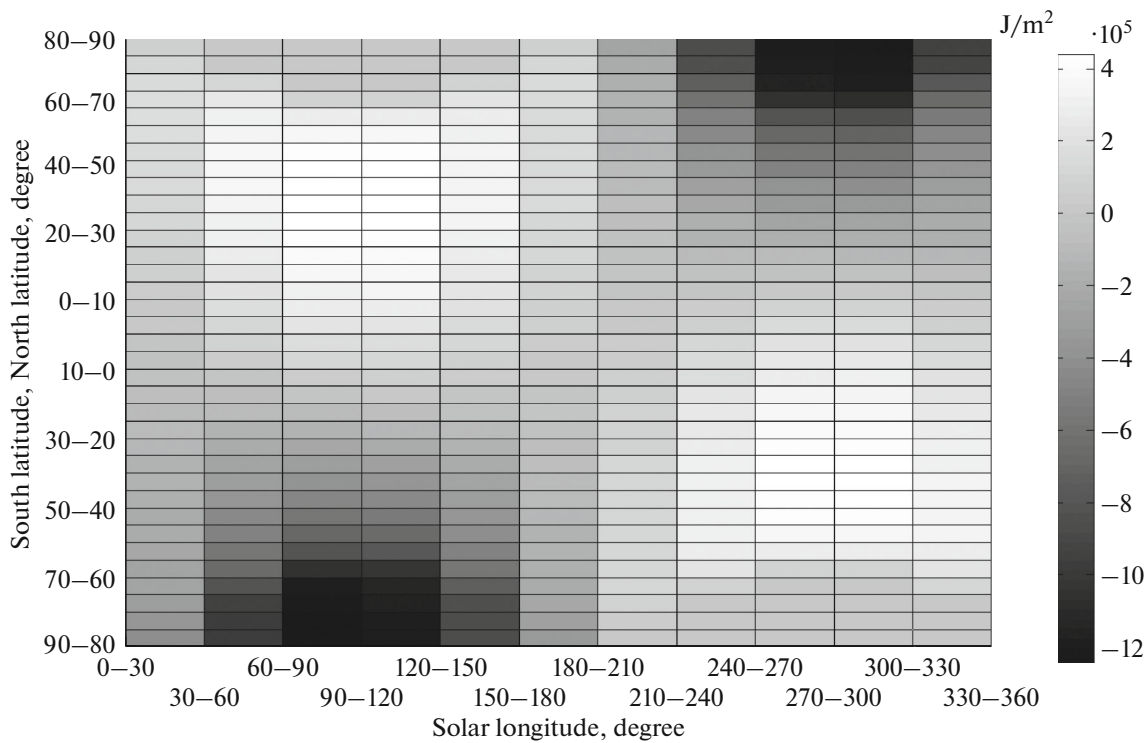


**Fig. 3.** Spatial and temporal changes in solar radiation arriving at the TOA for an astronomical month in the period from 1900 to 2100 (expressed in $J/m^2$).

of 70°−80° S, the incoming solar radiation is zero for the third to fourth astronomical months of a tropical year. To latitudinal zones of 80°−90° N and 70°−80° N, solar radiation does not come for the periods from the eighth to eleventh and from the ninth to tenth astronomical months, respectively. We call these regions "dead zones." No changes in the initial calculation conditions occur in these regions for the specified periods in the years 1900−2100.

(2) In a latitudinal zone of 0°−5° S, the increase in the incoming solar radiation is observed for all months of years 1900−2100.
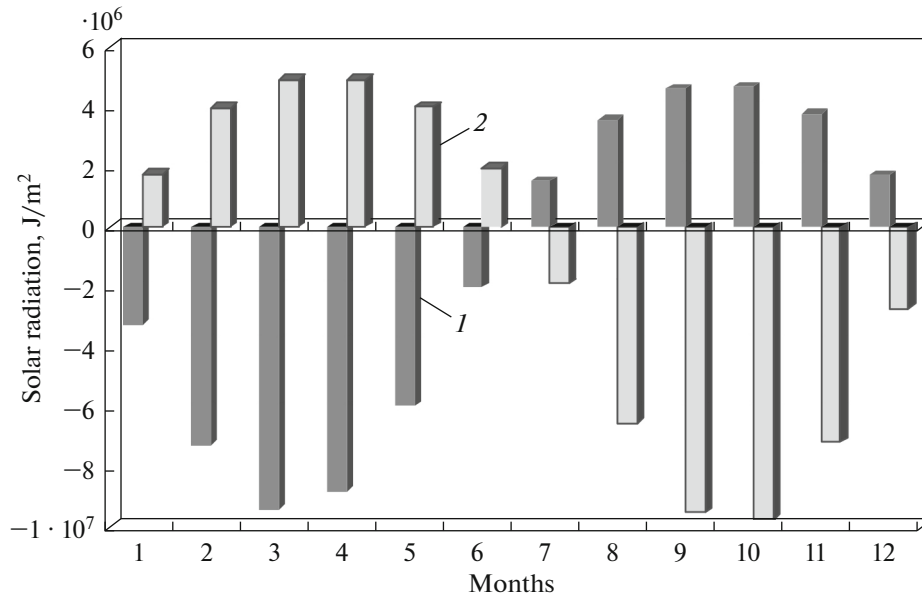
**Fig. 4.** The total change in solar radiation arriving at the TOA in the Northern (*1*) and Southern (*2*) Hemispheres for the period from 1900 to 2100.

(3) The decrease in solar radiation arriving at the TOA is characteristic of the summer 6-month periods, while the increase is characteristic for the winter ones. The reduction of solar radiation arriving at the TOA in both hemispheres becomes sequentially stronger when moving from the equatorial region to the poles. The increase in incoming solar radiation during the winter 6-month periods is more complex in character. In the Northern Hemisphere, growth is maximum during the ninth and tenth astronomical months in the latitudinal zone from 30° to 45° N. The absolute maximum in the increase of solar radiation coming to the Northern Hemisphere ($4.3603 \cdot 10^5$ J/m$^2$) is observed in the latitudinal zone from 40° to 45° N for the tenth astronomical month. In the Southern Hemisphere, the highest increase is regularly observed during the third and fourth months in a wider area, from 25° to 55° S (Fig. 3). The absolute maximum in the increase of incoming solar radiation is observed in the latitudinal zone from 40° to 45° S for the third astronomical month ($4.5130 \cdot 10^5$ J/m$^2$).

Thus, incoming radiation decreases in the polar regions. In general, for the years 1900−2100, the latitudinal contrast in solar radiation arriving at the TOA becomes stronger, while the seasonal differences are smoothed. This trend is determined by the decrease in the inclination of Earth's axis due to precession [4, 7, 13]. It is also noticed that the reduction of solar radiation arriving at the TOA during the summer 6-month periods is stronger than its growth in the winter 6-month periods (Fig. 4).

For 1900−2100, the total reduction of radiation arriving at the TOA in the Northern Hemisphere during the summer 6-month period is characterized by a value of $-3.6551 \cdot 10^7$ J/m$^2$. This is 0.541% of the average over the years 1900−2100 for the radiation coming to the TOA during the summer 6-month period in the Northern Hemisphere. During the winter 6-month period, solar radiation coming to the Northern Hemisphere increased by $1.9878 \cdot 10^7$ J/m$^2$ (0.495%). The solar radiation coming to the Southern Hemisphere increased by $2.1565 \cdot 10^7$ J/m$^2$ (0.554%) in the winter 6-month period, while it decreased by $-3.7401 \cdot 10^7$ J/m$^2$ (0.546%) in the summer 6-month period. Thus, secular spatial and temporal variations are observed in the solar radiation arriving at the TOA, which result in changes of the initial conditions for calculations of the energy balance. It is worth noting that changes in the semiannual and hemispheric insolation calculated for 1900−2100 exceed the known TSI variations in the 11-year cycle of solar activity (0.07%) [20].

Against the background of the revealed feature in the secular variability of solar radiation (Fig. 1), 19-year complicating variations are most pronounced. When determining the spatial structure of 19-year variations with a 1-year resolution, the calculations were simplified by analyzing the differences between the radiation coming in the tenth and first years of decades in the 1900−2100 period. According to our earlier results, the actual phases of the 19-year cycle are characterized by 8- and 11-year durations [7, 10, 11, 13]. These phases are formed by natural combinations of 2- and 3-year cycles (2 + 3 + 3 and 2 + 3 + 3 + 3), which are connected with the commensurability of the mean motions of Earth with Mars (2/1) and Venus (3/5). Thus, the Earth-to-Mars and Earth-to-Venus relative
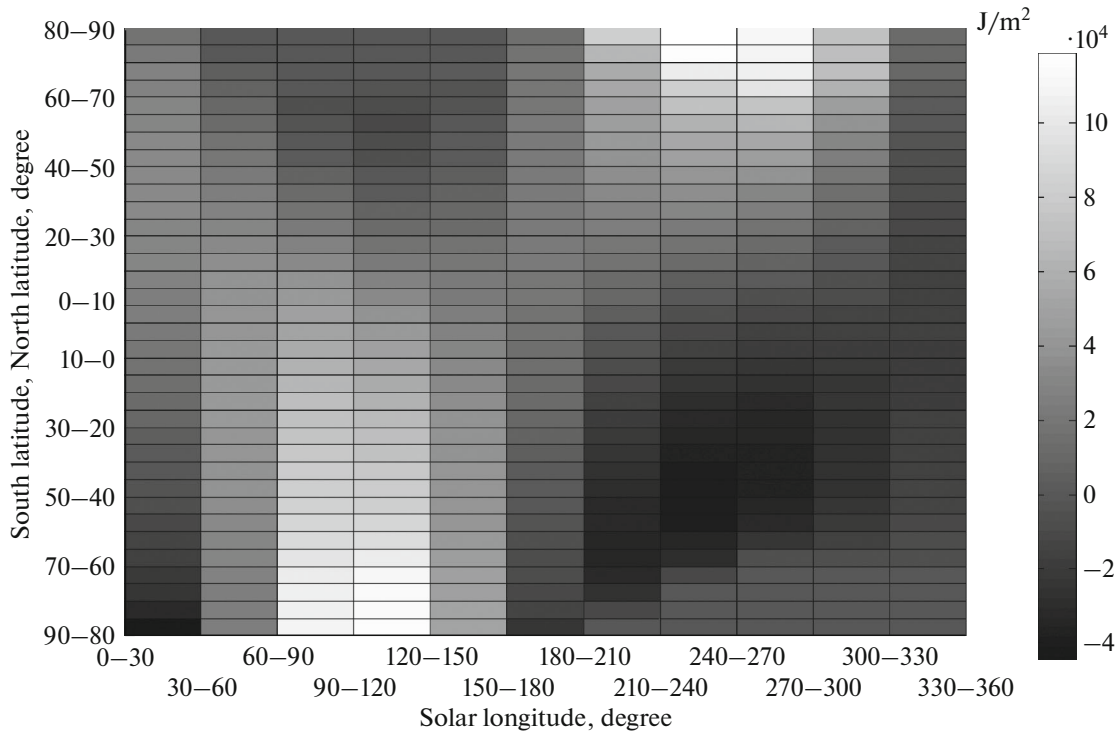
**Fig. 5.** Spatial and temporal changes in solar radiation arriving at the TOA in a phase of cycle 19 from 2012 to 2021.

positions with respect to the Sun repeat every 2 and 3 years, respectively. The alternating 11- and 8-year cycles calculated in the insolation series compose the 19-year cycle, which influences the trajectory, the velocity of the orbital motion of Earth, and the inclination of its rotation axis. Consequently, the variations caused by perturbations from the closest planets (Venus and Mars) are synchronous with the 19-year nutation cycle connected with Earth's satellite. These repetitions induce periodic resonance perturbations of the orbital motion of the Earth and, consequently, variations in the solar constant, the tropical year duration, and the energy coming to Earth for a tropical year.

The results show natural changes in the spatial and temporal structure of the incoming solar radiation in different phases of the 19-year cycle. Typically, in one phase of the cycle, solar radiation arriving at the TOA decreases during the summer 6-month period in a specified hemisphere and increases during the winter one (Fig. 5).

In the other phase of the cycle, an opposite situation is observed: incoming solar radiation decreases during winter 6-month periods and increases during the summer ones (Fig. 6).

Thus, one phase of the 19-year cycle strengthens the trend of the secular variability, while the other one weakens it. However, during 1900–2100, the regions, exhibiting a decrease or increase, significantly change in space (hemispheres) and time (6-month periods) in the phases of different 19-year cycles. For example, in

the 2012–2021 phase of the cycle, the decrease is mainly typical of the winter 6-month period in the Northern Hemisphere (Fig. 5). It is observed almost over the entire area of the hemisphere and amounts to $-1.6534 \cdot 10^6$ J/m$^2$ (0.041%) for the entire winter 6-month period. During the winter 6-month period in the Southern Hemisphere, the reduction of the incoming radiation is local. It is observed in a narrow spatial–temporal range; from the third to fifth astronomical months in the regions from 40° to 70° S. For this phase, during the summer 6-month period in the Northern Hemisphere, incoming radiation grows (except the first astronomical month in the latitudinal range from 40° to 90° N, where a reduction is detected). The total increase in solar radiation coming to the Northern Hemisphere for the summer 6-month period is 4.2448 J/m$^2$ (0.063%). During the summer 6-month period in the Southern Hemisphere, the total increase in the radiation coming at this phase of the cycle is 2.5143 J/m$^2$ (0.037%).

The other phase of the 19-year cycle, from 2021 to 2030, is expressed more distinctly (Fig. 6). At this phase, during the entire summer 6-month period in the Northern Hemisphere, a decrease in the solar radiation arriving at the TOA is detected. An exception is the first astronomical month (the increase is observed in the whole latitudinal range). At this phase, the total reduction of the incoming radiation during the summer 6-month period in the Northern Hemisphere is $-5.2707 \cdot 10^6$ J/m$^2$ (0.078%). During the
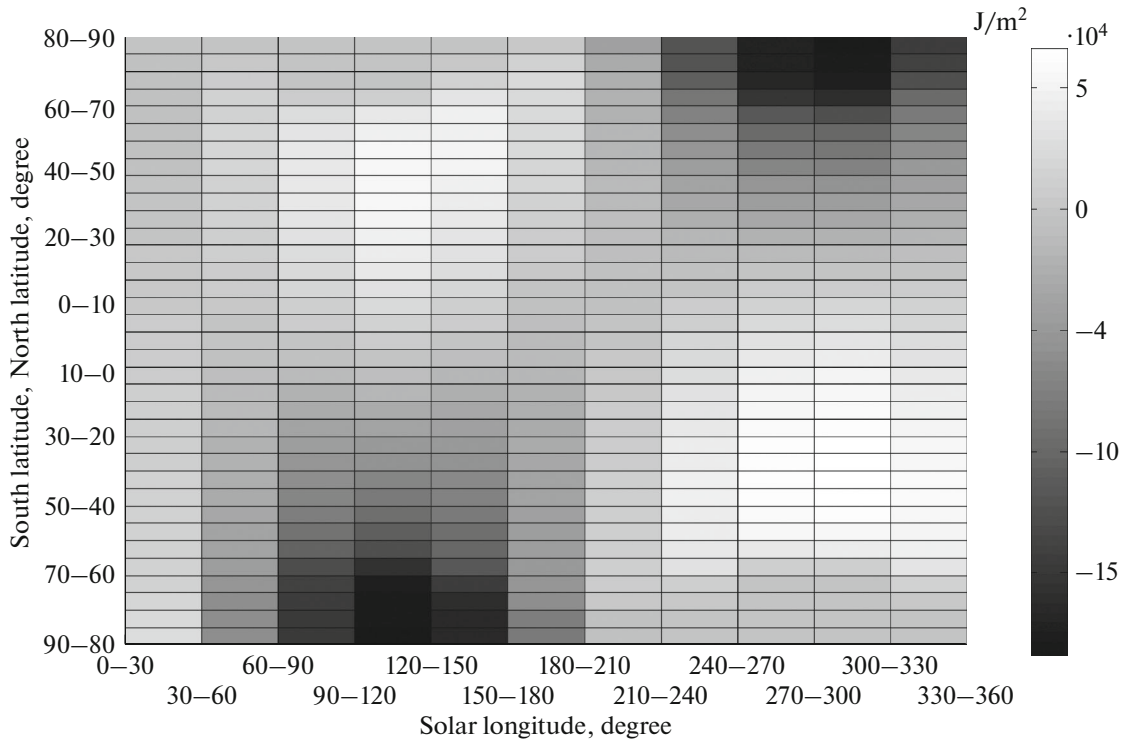
**Fig. 6.** Spatial and temporal changes in solar radiation arriving at the TOA in a phase of cycle 19 from 2021 to 2030.

winter 6-month period in the Northern Hemisphere, growth is detected (except in dead zones). The total increase is $2.9869 \cdot 10^6$ J/m$^2$ (0.074%). During the winter 6-month period in the Southern Hemisphere, solar radiation coming to the TOA increases (except in the $30°-85°$ range in the first astronomical month). At this phase, the total increase of the incoming radiation for this 6-month period is $1.7719 \cdot 10^6$ J/m$^2$ (0.044%). For the summer 6-month period in the Southern Hemisphere, the decrease is usual (except in the range $0°-15°$ in a period from the 8th to 12th astronomical month). The total decrease of solar radiation coming to the Southern Hemisphere for the summer 6-month period is $5.3149 \cdot 10^6$ J/m$^2$ (0.079%).

The detected variations in the insolation at the TOA in the phases of the 19-year cycle are approximately of the same order as the variations in the 11-year TSI cycle [20]. As for the 2-, 3-, 8-, and 11-year periodicity, it manifests itself by smaller amplitudes of spatial and temporal variability in solar radiation arriving at the TOA [7, 11].

## CONCLUSIONS

Based on astronomical ephemerides, the characteristics of spatial and temporal changes in solar radiation arriving at the TOA in the interval from 1900 to 2100 were calculated and their features were determined. It was found that the secular trend and the 19-year nutation-caused oscillation manifest them-

selves in the change of solar radiation arriving at the TOA. The secular trend reflects the increase in the solar radiation coming to a specified hemisphere during the winter 6-month periods and its decrease during the summer 6-month periods in this hemisphere. At the same time, one phase of the 19-year nutation cycle strengthens the secular trend, while the other one weakens it.

In calculations of the radiative and thermal balance of Earth and its surface and atmosphere, accounting for variations in solar radiation arriving at the TOA (i.e., changes in the initial conditions) may improve the calculation accuracy and the spatial−temporal resolution of the prognoses and their depth. The latter is connected with the fact that minor differences in the initial conditions may lead to the growing-in-time divergence in the calculation results, if the dependences are nonlinear. The obtained characteristics of the variations in solar radiation arriving at the TOA may improve the calculation accuracy and make the results of the analysis of the planetary energy disbalance more reliable [16, 22]. It is also possible to use the calculated values of solar radiation arriving at the TOA [19] in the physical and mathematical models of the climate.

## REFERENCES

1. Bakulin, P.I., Kononovich, E.V., and Moroz, V.I., *Kurs obshchei astronomii* (A Course of General Astronomy), Moscow: Nauka, 1983.

2. Budyko, M.I., *Izmenenie klimata* (Measurement of Climate), Leningrad: Gidrometeoizdat, 1974.

3. Drozdov, O.A., Vasil'ev, N.V., Raevskii, A.N., et al., *Klimatologiya* (Climatology), Leningrad: Gidrometeoizdat, 1989.

4. Milankovich, M., *Matematicheskaya klimatologiya i astronomicheskaya teoriya kolebanii klimata* (Mathematical Climatology and Astronomical Theory of Climate Fluctuations), Moscow−Leningrad: GONTI, 1939.

5. Monin, A.S., *Vvedenie v teoriyu klimata* (Introduction to the Climate Theory), Leningrad: Gidrometeoizdat, 1982.

6. Monin, A.S. and Shishkov, Yu.A., *Istoriya klimata* (History of Climate), Leningrad: Gidrometeoizdat, 1979.

7. Fedorov, V.M., *Insolyatsiya Zemli i sovremennye izmeneniya klimata* (The Earth's Insolation and Current Climate Changes), Moscow: Fizmatlit, 2018.

8. Khromov, S.P. and Petrosyants, M.A., *Meteorologiya i klimatologiya* (Meteorology and Climatology), Moscow: MGU, 2006.

9. Fedorov, V.M., Interannual variability of the solar constant, *Sol. Syst. Res.*, 2012, vol. 46, no. 2, pp. 170−176.
https://doi.org/10.1134/S0038094612020049

10. Fedorov, V.M., Interannual variations in the duration of the tropical year, *Dokl. Earth Sci.*, 2013, vol. 451, no. 1, pp. 750−753.
https://doi.org/10.1134/S1028334X13070015

11. Fedorov, V.M., Latitudinal variability of incoming solar radiation in various time cycles, *Dokl. Earth Sci.*, 2015, vol. 460, no. 1, pp. 96−99.
https://doi.org/10.1134/S1028334X15010183

12. Fedorov, V.M., Periodic perturbations and small variations of the solar climate of the earth, *Dokl. Earth Sci.*, 2014, vol. 457, no. 1, pp. 869−872.
https://doi.org/10.1134/S1028334X14070137

13. Fedorov, V.M., Spatial and temporal variation in solar climate of the earth in the present epoch, *Izv., Atmos. Ocean. Phys.*, 2015, vol. 51, no. 8, pp. 779−791.
https://doi.org/10.1134/S0001433815080034

14. Fedorov, V.M., Theoretical calculation of the interannual variability of the Earth's insolation with daily resolution, *Sol. Syst. Res.*, 2016, vol. 50, no. 3, pp. 220−224.
https://doi.org/10.1134/S0038094616030011

15. Giorgini, J.D., Yeomans, D.K., Chamberlin, A.B., et al., JPL's on-line solar system data service, *Bull. Am. Astron. Soc.*, 1996, vol. 28, no. 3, p. 1158.

16. Hansen, J., Sato, M., Kharecha, P., and von Schuckmann, K., Earth's energy imbalance and implications, *Atmos. Chem. Phys.*, 2011, vol. 11, no. 24, pp. 13421−13449.
https://doi.org/10.5194/acp-11-13421-2011

17. http://earthobservatory.nasa.gov/Features/EnergyBalance/page6.php.

18. http://ssd.jpl.nasa.gov.

19. http://www.solar-climate.com/sc/bd01.htm.

20. http://www.pmodwrc.ch/.

21. Kopp, G. and Lean, J., A new lower value of total solar irradiance: Evidence and climate significance, *Geophys. Res. Lett.*, 2011, vol. 37, L01706.
https://doi.org/10.1029/2010GL0455777

22. Loeb, N.G., Lyman, J.M., Johnson, G.C., et al., Observed changes in top-of-the-atmosphere radiation and upper-ocean heating consistent within uncertainty, *Nature Geosci.*, 2012, no. 5, pp. 110−113.
https://doi.org/10.1038/ngeo1375

23. Raschke, E. and Ohmura, A., Radiation budget of the climate system, in *Observed Global Climate, Landolt-Börnstein Group V Geophysics (Numerical Data and Functional Relationships in Science and Technology)*, Hantel, M., Ed., Berlin: Springer, 2005, vol. 6.

24. Stephens, G.L., Li, J., Wild, M., et al., An update on Earth's energy balance in light of the latest global observations, *Nature Geosci.*, 2012, vol. 5, pp. 691−696.
https://doi.org/10.1038/NGE01580

25. Trenberth, K.E. and Fasullo, J.T., Changes in the flow of energy through the Earth's climate system, *Meteorol. Z.*, 2009, vol. 18, no. 4, pp. 369−377.

26. Trenberth, K.E. and Fasullo, J.T., Tracking Earth's energy: From El Niño to global warming, *Surv. Geophys.*, 2012, vol. 33, nos. 3−4, pp. 413−426.
https://doi.org/10.1007/s10712-011-9150-2

27. Trenberth, K.E., Fasullo, J.T., and Kiehl, J., Earth's global energy budget, *Bull. Am. Meteorol. Soc.*, 2009, vol. 90, no. 3, pp. 311−323.
https://doi.org/10.1175/2008BAMS2634.1

*Translated by E. Petrova*